High Data Rate Ultrasonic Communications for Wireless Intra-body Networks

Emrecan Demirors*, Giovanni Alba†, G. Enrico Santagati*, Tommaso Melodia*
*Department of Electrical and Computer Engineering, Northeastern University, Boston, MA, USA
E-mail:{edemirors, santagati, melodia}@ece.neu.edu
†DEIB, Politecnico di Milano, Milano, Italy
E-mail:{giovanni.alba}@mail.polimi.it

***Abstract*—It is well known that electromagnetic radio-frequency (RF) waves that are the basis of most commercial wireless technologies are largely unsuitable to interconnect deeply implanted medical devices. RF waves are in fact absorbed by aqueous biological tissues and prone to malicious jamming attacks or to environmental interference from pervasively deployed RF communication systems; moreover, they pose a potential safety hazard when exposure of tissues is prolonged and at high power. While existing wireless technologies can satisfy the requirements of some specific applications, the root challenge of enabling networked intra-body miniaturized sensors and actuators that communicate through body tissues is largely unaddressed. Considering these limitations, this article proposes a high data rate *ultrasonic* communication scheme for wireless intra-body networks. The proposed scheme can enable various applications that require high sampling rates such as neural data recording or monitoring of the digestive tract through endoscopic pills. The proposed scheme is based on Orthogonal Frequency-Division Multiplexing (OFDM), which is proven to be robust against frequency-selective channels with relatively long delay spreads like the intra-body ultrasonic channel. The proposed scheme is implemented in a prototype ultrasonic software-radio and demonstrated to achieve data rates up to $28.12\,\mathrm{Mbit/s}$ through synthetic phantoms mimicking the ultrasonic propagation characteristics of biological tissues.**

***Keywords*—Ultrasonic communications, wireless intra-body networks, body area networks, high data rate ultrasonic communications, wireless neural recording.**

I. INTRODUCTION

Body area networking (BAN) is among the key technologies that will enable the *digital health* vision [1], whereby traditional clinical practice will be enhanced by and complemented with state-of-the-art advances in information technology. Among others, significant research efforts have been devoted to the development of miniaturized biomedical devices that can be implanted, ingested, or worn by humans and are wirelessly internetworked to collect diagnostic information and to fine-tune medical treatments over extended periods of time [2], [3]. This cross-fertilization between biomedical science and networking technology will enable and improve various applications including neural data recording and monitoring of the digestive tract through endoscopic pills, among others.

978-1-4673-9882-4/16/$31.00

Specifically, neural data recording has been an application of significant interest for neuroscientists. Its purpose is to monitor and record the neuronal electrical activity in the brain to investigate fundamentals of behavioral neuroscience and novel applications in neuroprosthetics. Today, most of the neuroprosthetics applications focus on (i) assisting tetraplegic patients to regain their capabilities of communicating and interacting with their environment through prosthetic devices (e.g., prosthetic arms) [4]–[6], (ii) enabling early diagnosis and prevention of neurological conditions, e.g., epilepsy and seizure [7], [8]. Neural data recording systems typically require high data rate communications (e.g., $24\,\mathrm{Mbit/s}$) because of the nature of data that are recorded continuously, at multiple sites, and with high sampling rates [9], [10]. Currently, the majority of existing BAN devices for neural data recording depend on traditional electromagnetic RF carrier waves. Similarly, endoscopic pills, which have been used for collecting images from the digestive system, mostly depends on RF carrier waves for enabling real-time wireless telemetry [11], [12]. In this paper, we contend that this is not the only possible approach, and that RF-based technologies have several limitations that can negatively affect the patients medical experience with neural data recording devices including:

- **High Absorption by tissues**. The human body is composed primarily (65%) of water. Therefore, RF waves are subject to high absorption, even at relatively low frequencies. For neural data recording systems, researchers have either designed implantable devices with relatively high transmission power levels [10], [13] that can potentially increase the temperature of the brain; or externally mounted devices [14], [15] that may decrease the comfort level of the patient. Similarly for endoscopic pills, researchers focused on lowering transmission power levels, which eventually limits the available data rates and accordingly the quality of the captured real-time video [11].
- **Crowded RF Spectrum.** The RF spectrum hosts a large (and increasing) number of devices that compete for spectrum access (e.g., WiFi, Bluetooth). Interference generated by such systems can affect the reliability and

security of the intra-body network, and ultimately the safety of the patient.

- **Safety Concerns.** In 2011, the the World the World Health Organization classified RF waves as possibly carcinogenic to humans [16]. Thus, a massive deployment of RF devices into the body, especially in proximity of delicate organs such as the brain, may raise safety concerns.
- **Interference.** RF communications are prone to jamming or eavesdropping caused by malicious agents using inexpensive and off-the-shelf devices. In many cases, jamming may not even be illegal on ISM spectrum frequencies where devices can transmit without any special permission.

In light of these formidable obstacles, in [17]–[19] we proposed a paradigm shift in wireless networking for implantable devices and explored the *use of ultrasonic waves to wirelessly internetworked intra-body devices*. Acoustic waves, which are typically generated through piezoelectric materials, are known to have better propagation characteristics than RF in dielectric media composed primarily of water [20]. Based on the medical experience of the last decades, ultrasonic waves are proved to be fundamentally safe as ultrasonic heat dissipation in tissues is minimal compared to RF [21] as far as acoustic power dissipation in tissue is limited to specific safety levels [2], [3]. Moreover, novel piezoelectric material and fabrication methods enable the production of miniaturized transducers at the micro [22] and even nano scales [23].

Orthogonal Frequency-Division Multiplexing (OFDM) is a communication scheme that has been widely used in underwater acoustic communications [24]–[27], due to its robustness against frequency-selective channels with long delay spreads. Considering that intra-body networks have channel characteristics to some extent similar to those of underwater acoustic networks, OFDM stands out as favorable signaling scheme to provide robust and high data rate communication links. Therefore, in this paper, we propose and demonstrate for the first time an Ultrasonic OFDM communication scheme that can support high data rate ultrasonic communications for intra-body networks, as required by applications such as neural data recording or wireless endoscopic pills. We demonstrate the capabilities of the proposed scheme through two sets of experiments on a software-defined testbed that consists of software-defined nodes communicating via ultrasonic waves through media that emulate acoustic propagation through biological tissues with high fidelity, i.e., ultrasonic phantoms. We experimentally prove the performance of the proposed scheme by showcasing data rates up to $28.12\,\mathrm{Mbit/s}$.

The remainder of the paper is organized as follows. In Section II we briefly review related work. In Section III we present the proposed Ultrasonic OFDM scheme. In Section IV we introduce the testbed architecture, while in Section V we extensively evaluate the performance of Ultrasonic OFDM. Finally, in Section VI we conclude the paper.

II. Related Work

In [2], [17], we showed that intra-body ultrasound propagation is severely affected by multipath caused by inhomogeneity of the body in terms of density, sound speed, and the pervasive presence of small organs and particles. In light of these observations, in [18] we proposed Ultrasonic Wide-Band (UsWB), a new ultrasonic multipath-resilient physical and medium access control (MAC) layer integrated protocol. UsWB is based on transmission of short carrierless ultrasonic pulses following a pseudo-random adaptive time-hopping pattern, with a superimposed adaptive spreading code. Thanks to impulsive transmission and spread-spectrum encoding UsWB is resilient against multipath and scattering effect and introduces waveform diversity among interfering nodes. Thus, it enables coexistence of multiple users on the same channel with limited interference. In [19], we experimentally showcased the feasibility of ultrasonic communications in human tissues by designing and building an FPGA-based prototype that incorporates the UsWB physical and medium access control protocols. We demonstrated that the proposed prototype can flexibly trade off data rate performance for power consumption, and achieve, for bit error rates (BER) no higher than, either (i) high-data rate transmissions up to $700\,\mathrm{kbit/s}$ at a transmit power of $-14\,\mathrm{dBm}$ ($40\,\mu\mathrm{W}$), or (ii) low-data rate and lower-power transmissions down to $-21\,\mathrm{dBm}$ ($8\,\mu\mathrm{W}$) at $70\,\mathrm{kbit/s}$ (in addition to numerous intermediate configurations). Moreover, we showed how the UsWB MAC protocol allows multiple concurrent users to coexist and dynamically adapt their transmission rate to channel and interference conditions to maximize throughput while satisfying predefined reliability constraints, e.g., maximum packet drop rate.

III. Ultrasonic OFDM

OFDM is a digital multicarrier signaling scheme that uses closely spaced orthogonal sub-carrier signals for conveying data on several parallel data channel, such that the channel on each subcarrier is subject to flat fading. In the time domain, this consists of dividing a high data rate stream into multiple low rate streams, each transmitted on a different subcarrier. In this way, the symbol rate on each subcarrier is reduced, and hence the effect of inter-symbol interference (ISI) caused by multipath delay spread is reduced. Considering this, we proposed OFDM communication schemes for underwater acoustic communications [24]–[26] to overcome the effect of frequency selective channels with long delay spreads. This paper reports on our efforts in designing and prototyping an OFDM signaling scheme for intra-body ultrasonic communications.

Specifically, in this paper, we define a packet format that consist of N consecutive OFDM blocks. To reduce the effect of multipath delay spread, we use a zero-padding (ZP) technique, which is based on padding zeros after each OFDM block to act as a guard interval. We chose ZP over other alternatives such as cyclic-prefixing (CP) because of its energy-efficiency. In the proposed packet format, each OFDM block is designed to have K subcarriers, which are assigned with three different roles: (i) K_D subcarriers are designated as data subcarriers for allocating data symbols, where each data symbol is a modulated version of information bits with different gray-coded modulation schemes (i.e., Binary-Phase-Shift-Keying (BPSK), Quadrature-Phase-Shift-Keying (QPSK), 8-PSK, 8-Quadrature-Amplitude-

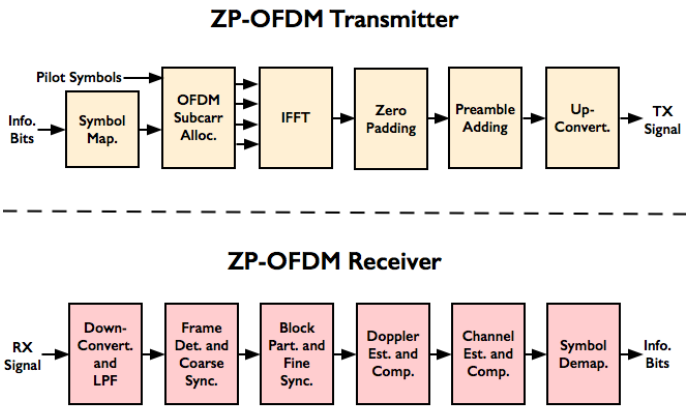

Fig. 1. Block diagrams of the ZP-OFDM transmitter and receiver.

Modulation (8-QAM), 16-QAM, 32-QAM, 64-QAM, 128-QAM); (ii) K_P subcarriers are charged as pilot subcarriers for carrying symbols that are known both by the transmitter and the receiver. Pilot subcarriers are equally spaced within the OFDM block and carry symbols that are mapped with BPSK for decreasing the complexity of the receiver algorithms [28]. The pilot subcarriers are exploited for performing channel estimation, block-level (fine) synchronization, and supporting Doppler scale estimation; (iii) K_N null subcarriers are assigned to be used for Doppler scale estimation. Moreover, the packet format includes a preamble, i.e., Pseudorandom-Noise (PN) sequence, preceding each packet for using in packet detection and coarse-synchronization operations.

Figure 1 shows the block diagram of the proposed OFDM scheme. At the transmitter side, the information bits are mapped into symbols based on the selected modulation scheme. The generated serial symbol stream is then converted into a parallel stream in accordance with the subcarrier positions alongside with pilot and null symbols. Consequently, the parallel stream is fed into an IFFT block, which outputs the symbol representations in the time domain as a serial stream. Later on, the a zero-padding operation is performed to generate ZP-OFDM blocks. The formed ZP-OFDM blocks are fed into an operational block, where they are transformed into the packet format with the addition of preamble block. Finally, the resulting stream is up-converted to the carrier frequency and transmitted. At the receiver side, first the received signal is down-converted to baseband and a low-pass filter (LPF) is used for filtering out the out-of-band noise and interference. The filtered baseband signals are then fed into synchronization blocks, where the correlation properties of the PN sequence are exploited to perform frame detection and coarse-synchronization. Following the coarse-synchronization, the OFDM frame is partitioned into individual OFDM blocks by performing the block-level synchronization by using the pilot symbols [27]. The partitioned OFDM blocks are then converted into parallel streams to be fed into the FFT block,

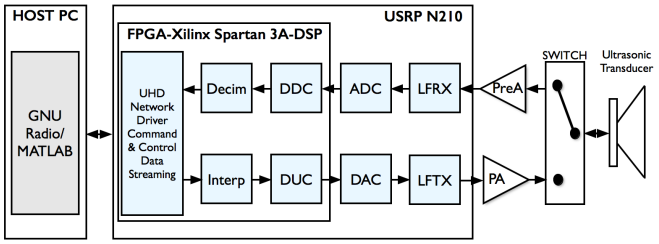

Fig. 2. The hardware architecture of the designed SDR-based node.

where they are converted to serial streams in the frequency domain. Later on, the frequency domain streams are passed to a block, where the Doppler scale is estimated and compensated accordingly. The Doppler-compensated OFDM blocks are fed into the a channel estimation block, which performs pilot-tone based channel estimation and channel equalization. Finally, a receiver block that incorporates a Zero-Forcing receiver maps equalized symbols onto the bits.

IV. Testbed Architecture

We implemented a custom software-based radio (SDR) based nodes for testing ultrasonic communication schemes, which we designed and used in our previous work [19]. Similar to [19], we built a testbed that consists of two of these SDR-based nodes, which support an ultrasonic communication link through an ultrasonic phantom that mimics the acoustic propagation properties of biological tissues with high fidelity. The custom SDR-based nodes consist of (i) a USRP N210, (ii) a host Linux-PC, (iii) a power amplifier/a voltage preamplifier, (iv) an electronic switch, and (v) an ultrasonic transducer. Fig. 2 depicts the hardware architecture of the node.

USRP N210. We selected USRP N210 [29], a commercially available, Field Programmable Gate Array (FPGA) based, SDR platform due to its low cost and wide adoption in academia and industry. USRP N210 consist of a motherboard and two daughterboards. Specifically in our node design, we selected LFTX and LFRX daughterboards, which cover a frequency band of (DC − 30 MHz) that enables a half-duplex transceiver operating in the ultrasonic frequency ranges of interest to us. The motherboard acts as the main processing unit, which is equipped with an analog-to-digital-converter (a dual 100 MS/s 14 − bit ADC) and a digital-to-analog-converter (a dual 400 MS/s 16 − bit DAC), that are both controlled by a 100 MHz master clock, and an FPGA unit (Xilinx Spartan 3A-DSP3400). The sampling rate of incoming digital samples (from ADC) and outgoing samples (to DAC) is fixed at 100 MS/s, while the FPGA digitally interpolates/decimates the sample stream to match the hardware sampling rate to the rate requested by the user. In USRP, high rate baseband signal processing is typically performed in an host-PC that is connected to the USRP through a Gigabit Ethernet (GigE) connection or in the FPGA.

Host Machine. The host machine is the processing unit that typically handles high rate baseband signal processing functionality. It can be either a desktop/laptop computer or

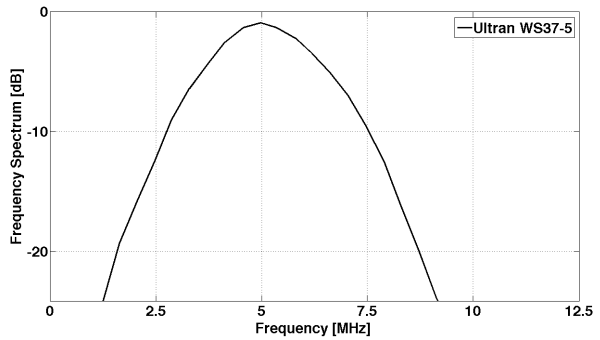

Fig. 3. Frequency response of the Ultran $\mathrm{WS37-5}$.

a computer-on-module, e.g., Gumstix, Raspberry Pi. To implement signal processing functionalities, we used GNU Radio [30], which is commonly used (i) to drive the USRP operations from the host-PC, (ii) as well as to implement signal processing operations in combination with MATLAB scripting language. GNU Radio provides a plethora of signal processing blocks that are implemented in C++ and that can be leveraged to rapidly implement a wide range of wireless communication schemes. In our testbed, we chose to use the GNU Radio framework because of its large set of available building blocks and because of the capability of creating new custom blocks easily for implementing customized communication schemes. In this paper, as explained in Section V, we also combine receiver functionalities of GNU Radio blocks and MATLAB scripting language for experiments.

Amplifiers and Switch. Our testbed uses amplifiers to enhance the communication range and performance of the ultrasonic link. At the transmitter side, we use a COTS power amplifier (PA), Mini-Circuits $\mathrm{LZY-22+}$ [31] that is capable of providing a gain of 43 dB across the operating frequency of $0.1-200$ MHz and leverage it to amplify the output power of the LFTX daughterboard (i.e., $2\,\mathrm{mW}$). At the receiver side, we use a COTS Low-Noise Amplifier (LNA), Mini-Circuits $\mathrm{ZFL-1000LN+}$ [32], which offers a low-noise figure of $2.9\,\mathrm{dB}$. To enable full-duplex operations with a single ultrasonic transducer on a time division basis, we incorporated in our node design a COTS electronic switch, Mini-Circuits $\mathrm{ZX80-DR230+}$, which offers a low insertion loss with a very high isolation over the frequency range of $0-3\,\mathrm{GHz}$. We drive the electronic switch by leveraging the General Purpose Input/Output (GPIO) digital pins available on the LFTX and LFRX daughterboards.

Ultrasonic Transducers. We use ultrasonic transducers that are capable of generating and detecting ultrasonic waves over a range of frequencies of interest to us. Typically, ultrasonic transducers are based on the piezoelectric effect, which enables two-way conversion between electrical and ultrasonic energy [33]. The main factors in determining the ultrasonic transducer to be used in the system is the operating frequency. It has been shown in [1] that while increasing the operating frequency allows to decrease the size of the transducer, it results in higher signal attenuation. Therefore, to be able to operate over the links that are in the order of several cm, the operating frequency should not exceed 10 MHz [2]. Moreover, today most of the biomedical sensing applications require directional transducers. Considering these, we aimed to select small-size directional ultrasonic transducers that can support lowest possible frequencies and large signal bandwidths. Hence, we used standard immersion ultrasonic transducers, Ultran $\mathrm{WS37-5}$ [34], which offers approximately a nominal bandwidth of $5\,\mathrm{kHz}$ at the central frequency of $5\,\mathrm{kHz}$. The frequency response of the Ultran $\mathrm{WS37-5}$ is illustrated in Fig. 3.

Fig. 4. SDR-based ultrasonic nodes are communicating through a human-kidney phantom.

Ultrasonic Phantoms. To emulate the intra-body ultrasonic communication channel with high fidelity, we used ultrasonic phantoms [35]. The ultrasonic phantoms consist of tissue-mimicking materials (tissue substitutes) that have the same acoustic propagation characteristics of human tissues, e.g., sound speed, density, and attenuation. Our testbed is based on an off-the-shelf human-kidney phantom immersed in a background water-based gel [36] that has the dimensions of $10\mathrm{cm}\times16\mathrm{cm}\times20\mathrm{cm}$. The background gel has the same density and sound speed as the kidney, which minimizes the possible reflections and retractions and accordingly can be considered acoustically transparent. The acoustic characteristics of the phantom are summarized in Table I.

TABLE I. ACOUSTIC CHARACTERISTICS OF THE ULTRASONIC PHANTOM

Tissue	Speed, v	Attenuation, α	Density, ρ
Background Gel	$1550\ \mathrm{m/s}$	$< 0.1\ \mathrm{dB/cm}$	$1020\ \mathrm{Kg/m^3}$
Kidney	$1550\ \mathrm{m/s}$	$2\ \mathrm{dB/cm}$ @ 5 MHz	$1030\ \mathrm{Kg/m^3}$

V. PERFORMANCE EVALUATION

In this section, we demonstrate the feasibility and the performance of the proposed ultrasonic communication scheme for intra-body communications through testbed experiments. We conducted two set of experiments on the testbed setup that consists of two SDR-based ultrasonic nodes communicating through a human-kidney phantom, as illustrated in Fig. 4. In the first set of experiments, we focused on realizing real-time implementation of the OFDM physical layer and evaluated its performance in terms of BER for different transmission power levels. In the second one, we concentrated on maximizing the data rate of the proposed scheme and evaluated results with offline processing.

A. Experiments with Real-Time Processing

In this set of experiments, we aim to reach a real-time implementation of the communication scheme that is defined

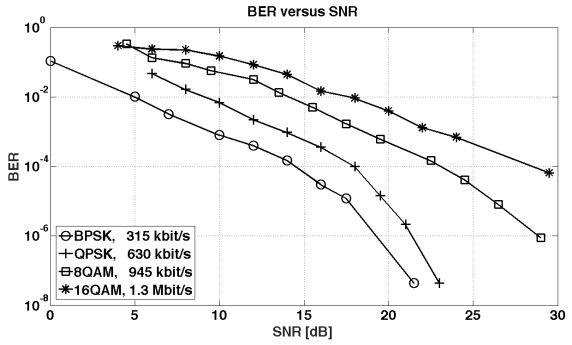

Fig. 5. BER versus SNR results for different modulation schemes.

in Section III. To obtain this, we designed and implemented all the processing blocks using GNU Radio on the host machine. However, the sampling rate and accordingly the data rate of this implementation are limited by two main factors: (i) the link capacity of the GigE connection between the host machine and the USRP that limits the maximum achievable sampling rate, i.e., $25\,\mathrm{MS/s}$. When this sampling rate is exceeded, the GigE connection starts experiencing network packet drops that cause loss of digital samples; (ii) purely software implementations (GNU Radio) of digital signal processing blocks introduce high processing latency [37]–[39], which eventually overloads the host machine when operating at high sampling rates, i.e., typically greater than $10\,\mathrm{MS/s}$. Therefore, if the host machine is not capable of processing the data as fast as the sampling rate, the internal buffers that store digital samples overflow and cause loss of digital samples.

To overcome this limitation, considering the processing time of our implementation, we limited our sampling rate to $781\,\mathrm{kS/s}$, which corresponds to a bandwidth of $390\,\mathrm{kHz}$. We used a carrier frequency of $5\,\mathrm{MHz}$, which matches with the center frequency of the ultrasonic transducers. We defined a packet structure that incorporates 32 OFDM blocks, each of them including 2048 total number of subcarriers and 128 pilot subcarriers. Each data subcarrier carries an information symbol that is mapped either with $BPSK, QPSK, 8QAM, 16QAM$. As a note, specifically for this set of experiments, we did not incorporate the power amplifier in the testbed setup.

Figure 5 shows BER versus SNR performance for different modulation schemes and accordingly different data rates. As expected, using a higher modulation scheme increases the data rate at the expense of BER performance. We observe that the proposed ultrasonic communication scheme can support data rates up to $1.3\,\mathrm{Mbit/s}$ at BER lower than 10^{-4} with real-time processing on the host machine.

B. Experiments with Offline Processing

In this set of experiments, our objective was to maximize the data rate of the ultrasonic communication scheme over the testbed setup. As explained in the Section V-A, a purely software implementation (GNU Radio) of the communication scheme limits the maximum data rate that can be reached. While it is possible to overcome this limitation by migrating software processing from the host machine to the FPGA to effectively speed up data processing and reduce the computational load on the host machine [19], [38], [39], such approach is beyond the scope of this paper. To that end, we performed offline experiments, where we have used GNU Radio only for recording the transmitted data while processing it offline with MATLAB.

We increased our sampling rate to $10\,\mathrm{MS/s}$, which translates into a bandwidth of $5\,\mathrm{MHz}$. Similar to the previous set of experiments, we used a carrier frequency of $5\,\mathrm{MHz}$. We used a packet structure that includes 32 OFDM blocks. Each of them has 32768 total number subcarriers and 2048 pilot subcarriers. Each data subcarrier conveys an information symbol that is mapped with higher order modulation schemes, i.e., $8QAM, 16QAM, 32QAM, 64QAM, 128QAM$.

Table II shows BER versus SNR performance for different modulation schemes and accordingly different data rates. We observe that data rates of $28.12\,\mathrm{Mbit/s}$ can be reached with a BER performance of 10^{-1} while data rates up to $20.12\,\mathrm{Mbit/s}$ are achievable with a BER lower than $3 * 10^{-2}$. As a note, in this specific set of experiments, we do not consider any forward-error-correction (FEC) coding, e.g., convolutional codes., that can trade off BER performance for data rate.

TABLE II. BER VERSUS SNR RESULTS FOR DIFFERENT MODULATION SCHEMES

Modulation	BER v	SNR [dB]	Data Rate [Mbit/s]
$8QAM$	$1.9 * 10{-}4$	17	12.09
$16QAM$	$5.8 * 10{-}3$	18	16.12
$32QAM$	$3.1 * 10{-}2$	13	20.15
$64QAM$	$8.0 * 10{-}2$	19	24.18
$128QAM$	$1.3 * 10{-}1$	20	28.12

VI. CONCLUSIONS

We designed a high data rate ultrasonic communication scheme for wireless intra-body networks. We discussed design and implementation of an OFDM communication scheme on a software-defined testbed architecture. We experimentally demonstrated the performance of the proposed communication scheme over synthetic phantoms mimicking the propagation characteristics of biological tissues. Specifically, we reached data rates up to $28.12\,\mathrm{Mbit/s}$, which can enable novel intra-body applications requiring high sampling rates such as neural data recording and wireless endoscopic pills.

ACKNOWLEDGEMENTS

This material is based upon work supported in part by the National Science Foundation under Grant CAREER CNS-1253309.

REFERENCES

[1] B. Latré, B. Braem, I. Moerman, C. Blondia and P. Demeester, "A Survey on Wireless Body Area networks," *ACM/Springer Wireless Networks*, vol. 17, no. 1, pp. 1–18, Jan. 2011.

[2] L. Galluccio, T. Melodia, S. Palazzo, and G. E. Santagati, "Challenges and Implications of Using Ultrasonic Communications in Intra-body Area Networks," in *Proc. of IEEE Intl. Conf. on Wireless On-demand Networked Systems (WONS)*, Courmayeur, Italy, Jan. 2012.

[3] T. Hogg and R. A. Freitas, "Acoustic Communication for Medical Nanorobots," *Nano Communication Networks (Elsevier)*, vol. 3, no. 2, pp. 83–102, Feb. 2012.

[4] L. R. Hochberg, M. D. Serruya, G. M. Friehs, J. A. Mukand, M. Saleh, A. H. Caplan, A. Branner, D. Chen, R. D. Penn, and J. P. Donoghue, "Neuronal ensemble control of prosthetic devices by a human with tetraplegia," *Nature*, vol. 442(7099), pp. 164–171, 2006.

[5] J. E. O'Doherty, M. A. Lebedev, P. J. Ifft, K. Z. Zhuang, S. Shokur, H. Bleuler, and M. A. L. Nicolelis, "Active tactile exploration using a brain-machine-brain interface," *Nature*, vol. 479(7372), pp. 228–231, Aug 2011.

[6] L. R. Hochberg, D. Bacher, B. Jarosiewicz, N. Y. Masse, J. D. Simeral, J. Vogel, S. Haddadin, J. Liu, S. S. Cash, P. der Smagt, and J. P. Donoghue, "Reach and grasp by people with tetraplegia using a neurally controlled robotic arm," *Nature*, vol. 485(7398), pp. 372–375, May 2012.

[7] W. Truccolo, J. A. Donoghue, L. R. Hochberg, E. N. Eskandar, J. R. Madsen, W. S. Anderson, E. N. Brown, E. Halgren, and S. S. Cash, "Single-neuron dynamics in human focal epilepsy," *Nature Neuroscience*, vol. 14(5), pp. 635–641, May 2011.

[8] M. A. Kramer and S. S. Cash, "Epilepsy as a disorder of cortical network organization," *Neuroscienctist*, vol. 18, pp. 360–372, 2012.

[9] A. V. Nurmikko, J. P. Donoghue, L. R. Hochberg, W. R. Patterson, Y. K. Song, C. W. Bull, D. A. Borton, F. Laiwalla, S. Park, Y. Ming, and J. Aceros, "Listening to brain microcircuits for interfacing with external world-progress in wireless implantable microelectronic neuroengineering devices," *Proceedings of the IEEE*, vol. 98, no. 3, pp. 375–388, March 2010.

[10] D. A. Borton, M. Yin, J. Aceros, and A. V. Nurmikko, "An implantable wireless neural interface for recording cortical circuit dynamics in moving primates," *Journal of Neural Engineering*, vol. 10, no. 2, 2013.

[11] B. Chi, J. Yao, S. Han, X. Xie, G. Li, and Z. Wang, "Low-power transceiver analog front-end circuits for bidirectional high data rate wireless telemetry in medical endoscopy applications," *IEEE Transactions on Biomedical Engineering*, vol. 54, no. 7, pp. 1291–1299, July 2007.

[12] M. R. Yuce and T. Dissanayake, "Easy-to-swallow wireless telemetry," *IEEE Microwave Magazine*, vol. 13, no. 6, pp. 90–101, Sept 2012.

[13] M. Rizk, C. A. Bossetti, T. A. Jochum, S. H. Callender, M. A. L. Nicolelis, D. A. Turner, and P. D. Wolf, "A fully implantable 96-channel neural data acquisition system," *Journal of Neural Engineering*, vol. 6, no. 2, p. 026002, 2009.

[14] H. Gao, R. M. Walker, P. Nuyujukian, K. A. A. Makinwa, K. V. Shenoy, B. Murmann, and T. H. Meng, "Hermese: A 96-channel full data rate direct neural interface in 0.13 μ m cmos," *IEEE Journal of Solid-State Circuits*, vol. 47, no. 4, pp. 1043–1055, April 2012.

[15] M. Yin, H. Li, C. Bull, D. A. Borton, J. Aceros, L. Larson, and A. V. Nurmikko, "An externally head-mounted wireless neural recording device for laboratory animal research and possible human clinical use," in *2013 35th Annual International Conference of the IEEE Engineering in Medicine and Biology Society (EMBC)*, July 2013, pp. 3109–3114.

[16] W. A. for Research on Cancer, "IARC classifies radio frequency electromagnetic fields as possibly carcinogenic to humans," May 2011. [Online]. Available: http://www.iarc.fr/en/media-centre/pr/2011/pdfs/pr208_E.pdf

[17] G. Santagati, T. Melodia, L. Galluccio, and S. Palazzo, "Ultrasonic networking for e-health applications," *IEEE Wireless Communications*, vol. 20, no. 4, pp. 74–81, 2013.

[18] ——, "Medium access control and rate adaptation for ultrasonic intra-body sensor networks," *IEEE/ACM Transactions on Networking*, vol. 23, pp. 1121–1134, August 2015.

[19] G. E. Santagati and T. Melodia, "Sonar Inside Your Body: Prototyping Ultrasonic Intra-body Sensor Networks," in *Proc. of IEEE Conf. on Computer Communications (INFOCOM)*, Toronto, Canada, April 2014.

[20] T. Melodia, H. Kulhandjian, L.-C. Kuo, and E. Demirors, "Advances in underwater acoustic networking," in *Mobile Ad Hoc Networking: Cutting Edge Directions*, S. Basagni, M. Conti, S. Giordano, and I. Stojmenovic, Eds. Hoboken, NJ: John Wiley & Sons, Inc., WSDHS 2012.

[21] A. Y. Cheung and A. Neyzari, "Deep local hyperthermia for cancer therapy: External electromagnetic and ultrasound techniques," *Cancer Res. (Suppl.)*, vol. 44, no. 9, pp. 4736–4744, Oct. 1984.

[22] G. Lockwood, D. Turnball, D. Christopher, and F. Foster, "Beyond 30 MHz [applications of high-frequency ultrasound imaging]," *IEEE Engineering in Medicine and Biology Magazine*, vol. 15, no. 6, Nov/Dec 1996.

[23] R. Smith, A. Arca, X. Chen, L. Marques, M. Clark, J. Aylott, and M. Somekh, "Design and fabrication of nanoscale ultrasonic transducers," *Journal of Physics: Conference Series*, vol. 353, no. 1, 2012.

[24] E. Demirors, G. Sklivanitis, G.E. Santagati, T. Melodia and S. N. Batalama, "Design of A Software-defined Underwater Acoustic Modem with Real-time Physical Layer Adaptation Capabilities," in *Proc. of ACM Intl. Conf. on Underwater Networks & Systems (WUWNet)*, Rome, Italy, November 2014.

[25] E. Demirors, B. G. Shankar, G.E. Santagati and T. Melodia, "SEANet: A Software-Defined Acoustic Networking Framework for Reconfigurable Underwater Networking," in *Proc. of ACM Intl. Conf. on Underwater Networks & Systems (WUWNet)*, Washington, DC, November 2015.

[26] E. Demirors, G. Sklivanitis, T. Melodia, S. N. Batalama, and D. A. Pados, "Software-defined underwater acoustic networks: Toward a high-rate real-time reconfigurable modem," *IEEE Communications Magazine*, vol. 53, no. 11, pp. 64–71, November 2015.

[27] S. Zhou and Z.-H. Wang, *OFDM for Underwater Acoustic Communications*. John Wiley and Sons, Inc., 2014.

[28] J. Rinne and M. Renfors, "Pilot spacing in orthogonal frequency division multiplexing systems on practical channels," *IEEE Transactions on Consumer Electronics*, vol. 42, no. 4, pp. 959–962, Nov 1996.

[29] "USRP Products," http://www.ettus.com.

[30] "GNU Radio," http://gnuradio.org/redmine/projects/gnuradio/wiki.

[31] "Mini-Circuits: LZY-22+ Datasheet," https://www.minicircuits.com/pdfs/LZY-22+.pdf.

[32] "Mini-Circuits: ZFL-1000LN+ Datasheet," http://www.minicircuits.com/pdfs/ZFL-1000LN+.pdf.

[33] K. K. Shung and M. Zippuro, "Ultrasonic transducers and arrays," *IEEE Engineering in Medicine and Biology Magazine*, vol. 15, no. 6, pp. 20–30, Nov 1996.

[34] "ULTRAN Group Transducers," http://www.ultrangroup.com/.

[35] M. O. Culjat, D. Goldenberg, P. Tewari, and R. S. Singh, "A review of tissue substitutes for ultrasound imaging," *Ultrasound in Medicine & Biology*, vol. 36, no. 6, pp. 861 – 873, 2010.

[36] "CIRS: Kidney Training Phantom," http://www.cirsinc.com/products/all/81/kidney-training-phantom/.

[37] K. R. Chowdhury and T. Melodia, "Platforms and testbeds for experimental evaluation of cognitive ad hoc networks," *IEEE Communications Magazine*, vol. 48, no. 9, pp. 96–104, Sept 2010.

[38] G. Nychis, T. Hottelier, Z. Yang, S. Seshan, and P. Steenkiste, "Enabling MAC protocol implementations on software-defined radios," in *Proceedings of USENIX Symp, on Networked systems design and implementation (NSDI)*, ser. NSDI'09, 2009, pp. 91–105.

[39] E. Demirors, G. Sklivanitis, T. Melodia, and S. N. Batalama, "RcUBe: Real-time reconfigurable radio framework with self-optimization capabilitites," in *Proc. of IEEE Intl. Conf. on Sensing, Communication, and Networking (SECON)*, Seattle, WA, June 2015.